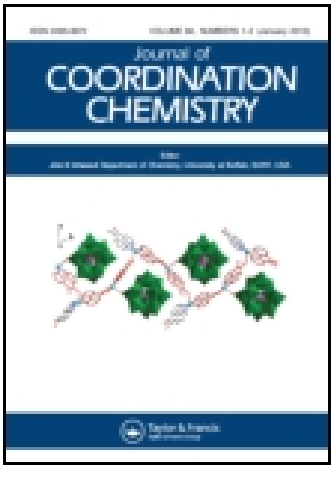

Journal of Coordination Chemistry
Publication details, including instructions for authors and subscription information:
http://www.tandfonline.com/loi/gcoo20

N-donor co-ligand-driven zinc coordination polymers based upon a bithiophene dicarboxylate: syntheses, structures, and luminescent properties

Tingting Cao[a], Jing Lu[a], Suna Wang[a], Changhui Zhou[a], Jianmin Dou[a], Dacheng Li[a] & Daqi Wang[a]

[a] Shandong Provincial Key Laboratory of Chemical Energy Storage and Novel Cell Technology, School of Chemistry and Chemical Engineering, Liaocheng University, Liaocheng, PR China

Accepted author version posted online: 10 Jun 2014.Published online: 15 Jul 2014.

To cite this article: Tingting Cao, Jing Lu, Suna Wang, Changhui Zhou, Jianmin Dou, Dacheng Li & Daqi Wang (2014) N-donor co-ligand-driven zinc coordination polymers based upon a bithiophene dicarboxylate: syntheses, structures, and luminescent properties, Journal of Coordination Chemistry, 67:11, 1948-1961, DOI: 10.1080/00958972.2014.933211

To link to this article: http://dx.doi.org/10.1080/00958972.2014.933211

Journal of Coordination Chemistry, 2014
Vol. 67, No. 11, 1948–1961, http://dx.doi.org/10.1080/00958972.2014.933211

N-donor co-ligand-driven zinc coordination polymers based upon a bithiophene dicarboxylate: syntheses, structures, and luminescent properties

TINGTING CAO, JING LU, SUNA WANG*, CHANGHUI ZHOU, JIANMIN DOU, DACHENG LI* and DAQI WANG

Shandong Provincial Key Laboratory of Chemical Energy Storage and Novel Cell Technology, School of Chemistry and Chemical Engineering, Liaocheng University, Liaocheng, PR China

(*Received 21 February 2014; accepted 16 May 2014*)

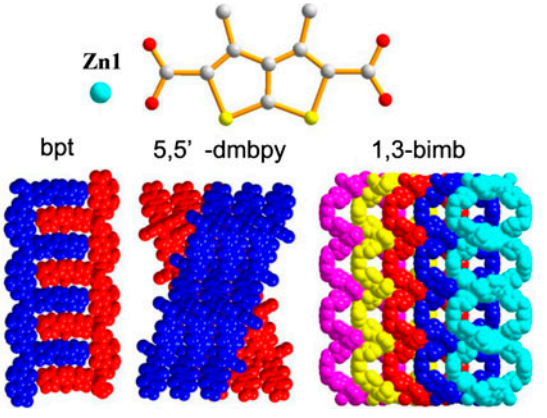

Three zinc coordination compounds were hydrothermally obtained from a scarcely investigated bithiophene dicarboxylate acid. The N-donor co-ligands have a large effect on the resulting structures. The compounds and ligands exhibit photoluminescent properties at room temperature.

Three zinc compounds assembled from a bithiophene dicarboxylic acid (H_2DMTDC) and different N-donor co-ligands, $[Zn(DMTDC)(bpt)(H_2O)]_n$ (**1**), $\{[Zn(DMTDC)(5,5\text{-dmbpy})]\cdot 0.5DMF\cdot 1.5H_2O\}_n$ (**2**), and $\{[Zn(DMTDC)(1,3\text{-bimb})]\cdot 2DMF\cdot H_2O\}_n$ (**3**) (H_2DMTDC = 3,4-dimethylthieno[2,3-*b*]thiophene-2,5-dicarboxylic acid, bpt = 4-amino-3,5-bis(4-pyridyl)1,2,4-triazole, 5,5′-dmbpy = 5,5′-dimethyl-2,2′-bipyridyl, 1,3-bimb = 1,3-bis(imidazol-1ylmethyl)benzene), were solvothermally synthesized and characterized. Compounds **1** and **2** are 1-D linear and zigzag chains with different supramolecular structures. In **1**, adjacent chains form zipper-like structures through N–H···N interactions. In **2**, however, chains in adjacent layers are stacked in an unusual unparallel level through C–H···O interactions. Compound **3** features a highly corrugated 2-D (4,4) layer and the layers are penetrated by

*Corresponding authors. Email: wangsuna@lcu.edu.cn (S. Wang); lidacheng@lcu.edu.cn (D. Li)

each other to give 3-D polycatenations. Right- and left-handed helical Zn-bimb chains are arranged alternately within and between the layers, leading to mesomeric property of the whole network. Thermal stability and the decomposed products of all compounds were investigated. Luminescent properties of the ligands and compounds in the solid state at room temperature have also been explored. Moreover, the luminescence intensities of the compounds in different solvents are largely dependent on the solvent.

Keywords: Zinc; Coordination polymer; 3,4-Dimethylthieno[2,3-*b*]thiophene-2,5-dicarboxylic acid; N-Donor co-ligands

1. Introduction

Coordination polymers have been researched extensively stemming from both fascinating architectures and potential applications including luminescence, magnetism, gas storage, etc. [1, 2]. As essential construction units, organic ligands are important to the assembly of these compounds. O- and N-containing ligands, especially aromatic multicarboxylates and N-containing heterocyclic ligands, have been widely employed for their various coordination modes and strong affinities for transitional metal ions [3–8]. Only a few *S*-containing carboxylic ligands, however, have been reported. Limited investigation is mostly focused on thiophene dicarboxylic acid (H_2tda) [9–13]. Several compounds have been reported from bithiophendicarboxylic acids, such as thieno[3,2-b]thiophene-2,5-dicarboxylic acid [14], 2,2′-bithiophene-5,5′-dicarboxylic acid [15, 16], 2,6-dithieno[3,2-b:2′,3′-d]thiophenedicarboxylic acid [17], and dithieno[3,2-b:2′,3′-e]benzene-2,6-dicarboxylic acid [18]. Su *et al.* have recently reported two metal–organic frameworks based on 3,4-dimethylthieno[2,3-b] thiophene-2,5-dicarboxylic acid (H_2DMTDC), which have been applied as a chromatographic column for separating transition metal ions [19]. The structures and properties of these thiophene-based derivatives vary considerably depending on the π-conjugation modes at the thiophene subunits and may be a highly promising platform for construction of a new class of materials.

Our research is focused on the coordination chemistry of multicarboxylic acids. A series of coordination compounds have been constructed from several aromatic multicarboxylic acids, such as *N*,*N*′,*N*″-1,3,5-triazine-2,4,6-triyltrisglycine) [20], 2,2′,2″-[1,3,5-triazine-2,4,6-triyltris(thio)]tris-acetic acid [21], *N*,*N*′,*N*″-tris(carboxymethyl)-1,3,5-benzenetricarboxamide [22], and 4,4′-methylenebis(3-hydroxy-2-naphthalenecarboxylic acid [23]. Herein, we report three zinc coordination compounds based on 3,4-dimethylthieno[2,3-b]thiophene-2,5-dicarboxylic acid (H_2DMTDC). By introducing different N-donor co-ligands, 4-amino-3,5-bis (4-pyridyl)-1,2,4-triazole (bpt), 5,5′-dimethyl-2,2′-bipyridyl (5,5′-dmbpy), and 1,3-bis(imidazol-1-ylmethyl)benzene (1,3-bimb), three zinc coordination polymers, $[Zn(DMTDC)(bpt)(H_2O)]_n$ (**1**), $\{[Zn(DMTDC)(5,5'\text{-dmbpy})]\cdot 0.5DMF\cdot 1.5H_2O\}_n$ (**2**), and $\{[Zn(DMTDC)(1,3\text{-bimb})]\cdot 2DMF\cdot H_2O\}_n$ (**3**), were hydrothermally synthesized. **1** and **2** are 1-D chains with different supramolecular structures. In **1**, adjacent chains form zipper-like structures through N–H···N interactions. In **2**, however, neighboring chains in adjacent layers are stacked in unparallel directions. **3** features a highly corrugated 2-D (4,4) layer with right- and left-handed helical Zn-bimb chains arranged alternately and the layers are penetrated by each other to give 3-D polycatenations. Luminescent properties of the compounds at room temperature have been explored.

2. General methods

H_2DMTDC was synthesized according to previous report [24]. Other reagents were commercially available and used as purchased without purification. Elemental analyses were carried out with a Perkin-Elmer 240C elemental analyzer. FT-IR spectra were recorded as KBr pellets from 4000 to 400 cm^{-1} on a VECTOR 22 spectrometer. Powder X-ray diffraction (PXRD) data were collected over the 2θ range 5–50° on a Philips X'pert diffractometer using Cu-Kα radiation ($\lambda = 1.5418$ Å) at room temperature. Thermal analyses were performed on a thermogravimetric analysis (TGA) V5.1A Dupont 2100 instrument from room temperature to 700 °C with a heating rate of 10 °C min^{-1} under flowing nitrogen. The emission/excitation spectra were recorded on a Hitachi 850 fluorescence spectrophotometer.

2.1. *Synthesis of [Zn(DMTDC)(bpt)(H_2O)]$_n$ (1)*

A mixture of H_2DMTDC (0.025 g, 0.1 mM), $Zn(NO_3)_2 \cdot 6H_2O$ (0.030 g, 0.1 mM) and bpt (0.008 g, 0.05 mM) in H_2O (6 mL) and DMF (6 mL) was placed in a Parr Teflon-lined stainless steel vessel and heated to 80 °C for 2 days. Then, the reaction system was cooled to room temperature slowly and brown block crystals of **1** were obtained. After filtration, the crystals were washed with water and dried in air (0.017 g, yield 29.5% based on H_2DMTDC). Anal. Calcd for $C_{22}H_{18}N_6O_5S_2Zn$ (**1**): C, 45.84; H, 3.12; N, 14.58. Found: C, 45.71; H, 3.19; N, 14.49. IR (KBr pellet, cm^{-1}): 3339(vsbr), 1622(vs), 1498(s), 1461(m), 1371(m), 1333(s), 1223(m), 1113(w), 1069(w), 1026(m), 975(w), 824(w), 742(m), 698(m), 628(w), 504(w).

2.2. *Synthesis of [Zn(DMTDC)(5,5′-dmbpy)]·0.5DMF·1.5H_2O}$_n$ (2)*

Similar procedures to **1** were performed to obtain colorless crystals of **2**, except that 5,5′-dmbpy was used instead of bpt (0.028 g yield 47.3% based on H_2DMTDC). Anal. Calcd for $C_{25.5}H_{24.5}N_{2.5}O_6S_2Zn$ (**2**): C, 51.74; H, 4.14; N, 5.92. Found: C, 51.64; H, 4.18; N, 5.87. IR (KBr pellet, cm^{-1}): 3440(vsbr), 1676(vs), 1594(m), 1568(m), 1499(s), 1482(m), 1380(s), 1371(m), 1359(s), 1147(w), 1089(m), 1046(m), 975(w), 924(w), 839(m), 820(m), 786(m), 657(w), 539(w).

2.3. *Synthesis of {[Zn(DMTDC)(1,3-bimb)]·2DMF·H_2O}$_n$ (3)*

Similar procedures to **1** were performed to obtain colorless crystals of **3**, except that 1,3-bimb was used instead of bpt (0.019 g, yield 26.3% based on H_2DMTDC). Anal. Calcd for $C_{30}H_{36}N_6O_7S_2Zn$ (**3**): Calcd C, 49.85; H, 4.98; N, 11.63. Found: C, 49.80; H, 4.92; N, 11.67. IR (KBr pellet, cm^{-1}): 3450(vsbr), 1663(vs), 1610(m), 1524(w), 1383(m), 1365(m), 1339(m), 1239(w), 1093(w), 1025(w), 952(w), 924(w), 813(m), 787(m), 728(m), 657(m).

3. X-ray crystallography

Suitable single crystals of **1–3** selected for indexing and intensity data were measured on a Siemens Smart CCD diffractometer with graphite-monochromated Mo-Kα radiation

Table 1. Crystal data and structure refinement information for **1–3**.

Compound	**1**	**2**	**3**
Formula	$C_{24}H_{18}N_2O_4S_2Zn$	$C_{22}H_{18}N_6O_5S_2Zn$	$C_{30}H_{36}N_6O_7S_2Zn$
Formula weight	527.89	575.91	722.14
T (K)	293(2)	293(2)	293(2)
Crystal system	Orthorhombic	Monoclinic	Orthorhombic
Space group	*Pnna*	*C2/c*	*Pbca*
a (Å)	15.7431(5)	24.8708(8)	14.2691(4)
b (Å)	21.6956(6)	12.3386(3)	21.0560(6)
c (Å)	7.6456(4)	14.7957(5)	23.3214(6)
α (°)	90	90	90
β (°)	90	97.269(3)	90
γ (°)	90	90	90
V (Å^3)	2611.40(18)	4503.9(2)	7006.9(3)
Z	4	8	8
D_{Calcd} (g cm^{-3})	1.343	1.699	1.369
μ (mm^{-1})	1.130	1.327	0.872
θ Range	2.59–25.02	2.98–25.02	2.56–25.02
Index ranges	$-18 \le h \le 18$	$-29 \le h \le 25$	$-16 \le h \le 16$
	$-25 \le k \le 23$	$-14 \le k \le 14$	$-25 \le k \le 25$
	$-9 \le l \le 9$	$-17 \le l \le 17$	$-27 \le l \le 26$
R_1; wR_2[a] [$I > 2\sigma(I)$]	0.0627; 0.1875	0.0345; 0.0743	0.0647; 0.1787
GOOF	1.037	1.044	1.028

[a]$R_1 = \sum||F_o|-|F_c||/|F_o|$. $wR_2 = [\sum w(\sum F_o^2 - F_c^2)^2/\sum w(F_o^2)^2]^{1/2}$

Table 2. Selected bond lengths (Å) and angles (º) of **1–3**.

Compound **1**			
Zn(1)–O(1A)	1.969(4)	Zn(1)–O(1)	1.969(4)
Zn(1)–N(1)	2.075(5)	Zn(1)–N(1A)	2.075(5)
O(1A)–Zn(1)-O(1)	120.2(3)	O(1A)–Zn(1)–N(1)	97.7(2)
O(1)–Zn(1)–N(1)	129.32(19)	O(1A)–Zn(1)–N(1A)	129.32(19)
O(1)–Zn(1)–N(1A)	97.7(2)	N(1)–Zn(1)–N(1A)	79.4(3)
O(1A)–Zn(1)–C(1A)	28.5(2)		
Compound **2**			
Zn(1)–O(4A)	1.9320(19)	Zn(1)–O(1)	1.9442(19)
Zn(1)–O(5)	1.991(2)	Zn(1)–O(5)	1.991(2)
Zn(1)–N(1)	2.056(2)	O(4)–Zn(1) (B)	1.9320(19)
O(4A)–Zn(1)–O(1)	144.95(10)	O(4A)–Zn(1)–O(5)	105.02(8)
O(1)–Zn(1)–O(5)	103.15(8)	O(4A)–Zn(1)–N(1)	94.71(9)
O(1)–Zn(1)–N(1)	98.10(9)	O(5)–Zn(1)–N(1)	104.37(9)
Compound **3**			
Zn(1)–O(4A)	1.987(3)	Zn(1)–O(1)	1.993(3)
Zn(1)–O(1)	1.993(3)	Zn(1)–N(1)	2.030(4)
Zn(1)–N(4B)	2.034(4)	O(4)–Zn(1-D)	1.987(3)
O(4A)–Zn(1)–N(1)	102.95(15)	O(4A)–Zn(1)–O(1)	130.92(15)
O(1)–Zn(1)–N(1)	107.67(16)	O(4A)–Zn(1)–N(4B)	104.54(15)
O(1)–Zn(1)–N(4B)	101.41(15)		

Notes: Symmetry codes: **1**, A, x, $-y+1/2$, $-z+3/2$; **2**, A, x, $y+1$, z, B, x, $y-1$, z; **3**, A, $-x+1/2$, $y-1/2$, z; B, x, $-y+1/2$, $z+1/2$; C, x, $-y+1/2$, $z-1/2$; D, $-x+1/2$, $y+1/2$, z.

($\lambda = 0.71073$ Å) at 298 K. The raw data frames were integrated into SHELX-format reflection files and corrected using SAINT [25]. Absorption corrections based on multiscan were obtained by SADABS [26]. The structures were solved with direct methods and refined with full-matrix least-squares method using the SHELXS-97 and SHELXL-97

programs [27], respectively. Displacement parameters were refined anisotropically and the positions of hydrogens were generated geometrically, assigned isotropic thermal parameters, and allowed to ride on their parent carbons before the final cycle of refinement. In **2**, atoms of the thiophene ring are disordered over two general positions (C3/C3′, C4/C4′, C5/C5′, C6/C6′, S1/S1′), which were refined isotropically with a site-of-occupancy of 0.50/0.50. The lattice DMF and H_2O molecules are disordered. The SQUEEZE program was used to remove scattering from these highly disordered solvent molecules and a new .HKL file was generated. The structure was solved by using the new .HKL file [28]. Details regarding the crystals and structure determination are provided in table 1, and selected bond lengths and angles are listed in table 2.

4. Description of the structures

4.1. *Description of [Zn(DMTDC)(bpt)(H_2O)]$_n$ (1)*

X-ray diffraction (XRD) indicated that **1** crystallizes in the space group *C2/c* with the crystal system of monoclinic and exhibits a 1-D chain structure. As shown in figure 1(a), the asymmetric unit consists of one Zn(II), one $DMTDC^{2-}$, one bpt, and one coordinated water. The Zn(II) ion adopts four-coordinate tetrahedral geometry with two carboxylate oxygens (O1 and O4A) from two different $DMTDC^{2-}$ ligands, one pyridine nitrogen (N1) from bpt and one water (O5). The Zn–O and Zn–N bond lengths lie in the normal range of 1.932 (2)–2.056(2) Å. The $DMTDC^{2-}$ adopts the $(\kappa^1\text{-}\kappa^0)\text{-}(\kappa^1\text{-}\kappa^0)\text{-}\mu_2$ mode, connecting Zn(II) ions into 1-D linear arrays along the *b*-axis with the terminal bpt ligands decorated on the same side of the chain [figure 1(b)]. The adjacent intrachain Zn···Zn distance is 12.3386(6) Å. From the topological view, the coordinated water could be omitted and each Zn(II) ion viewed as a three-connected T-shaped node. As a consequence, the extension of such T-shaped nodes results in the formation of a 1-D chain motif with grooves. The linear arrays display a unique packing structure. As depicted in figure 1(c), the dangling bpt ligands from one chain interdigitate into the grooves of a neighboring chain through N–H···N and N–H···S interactions existing between amino nitrogen (N6) and thiophene sulfur (S1), resulting in a zipper-like structure. These zippers are further connected through O–H···O interactions between the coordinated water (O5) and uncoordinated carboxylate oxygens (O2 and O3), forming a 2-D layer along the *ac* plane. The overall 3-D supramolecular structure is formed through $\pi\cdots\pi$-stacking interactions between aromatic rings (figure S1, see online supplemental material at http://dx.doi.org/10.1080/00958972.2014.933211).

4.2. *Description of [Zn(DMTDC)(5,5′-dmbpy)]·0.5DMF·1.5H_2O}$_n$ (2)*

Compound **2** crystallizes in the space group *Pnna* with orthorhombic crystal system and also displays a 1-D chain structure. As described in figure 2(a), the asymmetric unit consists of half of a Zn(II) ion, half of a disordered $DMTDC^{2-}$, and half of a 5,5′-dmbpy. The Zn (II) adopts four-coordinate tetrahedral geometry with two carboxylate oxygens (O1 and O1A) from two different $DMTDC^{2-}$ ligands and two nitrogens (N1 and N1A) of chelating 5,5′-dmbpy. The Zn–O and Zn–N bond lengths are normal, 1.969(4)–2.075(5) Å. The $DMTDC^{2-}$ also adopts the $(\kappa^1\text{-}\kappa^0)\text{-}(\kappa^1\text{-}\kappa^0)\text{-}\mu_2$ mode, connecting Zn(II) ions into 1-D zigzag chains along the *b*-axis with 5,5′-dmbpy at each node at the same side [figure 2(b)]. The

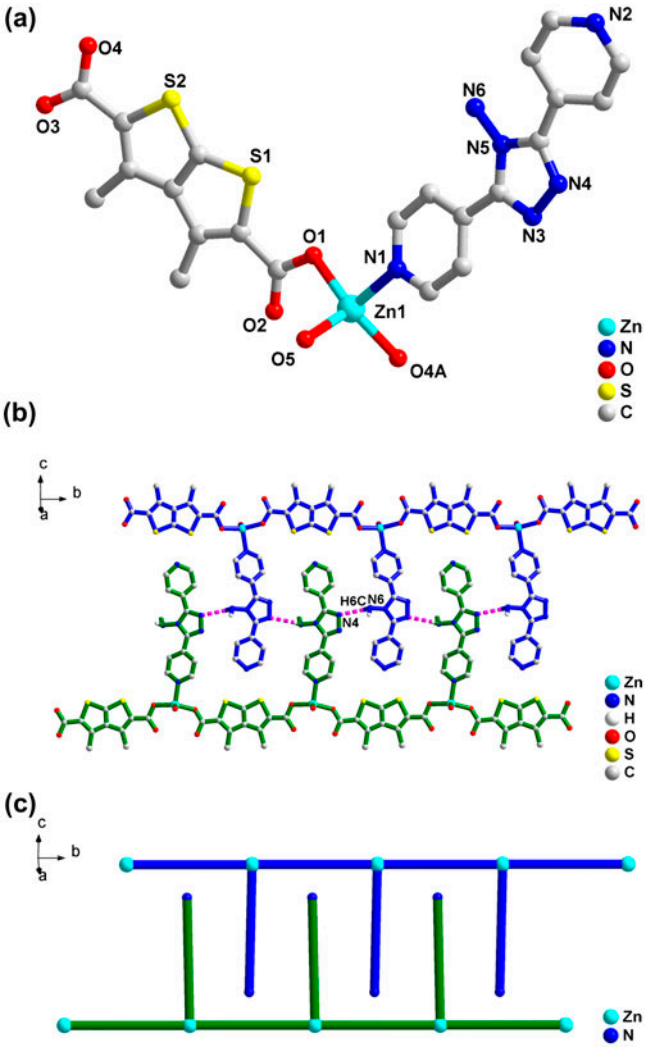

Figure 1. (a) Local coordination environment of **1**. All hydrogens are omitted for clarity. Symmetry codes for the generated atoms: A: x, $1+y$, z. (b) View of weak interactions between the adjacent chains along the b-axis. (c) View of the topological representation of the zipper-like structures based on T-shaped nodes.

Zn···Zn distance within the chain is 12.3386(6) Å. Hydrogen (H9) on C9 of the pyridine ring of 5,5′-dmbpy and coordinated carboxylate oxygen O1 form C–H···O interactions, extending these chains into the overall 3-D supramolecular structure [figure 2(c)]. The C···O distance and C–H···O angle are 3.325(10) Å and 163.4(5)°, respectively. The chains in adjacent layers exhibit interesting arrangement through stacking in two different directions, not parallel as in normal chain structures [figure 2(d)]. Through this special packing mode, 1-D channels along the a-axis are generated which are filled with disordered DMF and H_2O molecules (figure S2). The potential solvent-accessible volume in the unit cell is 574.9 $Å^3$, which accounts for 22.0% of the total cell volume as calculated by PLATON [28].

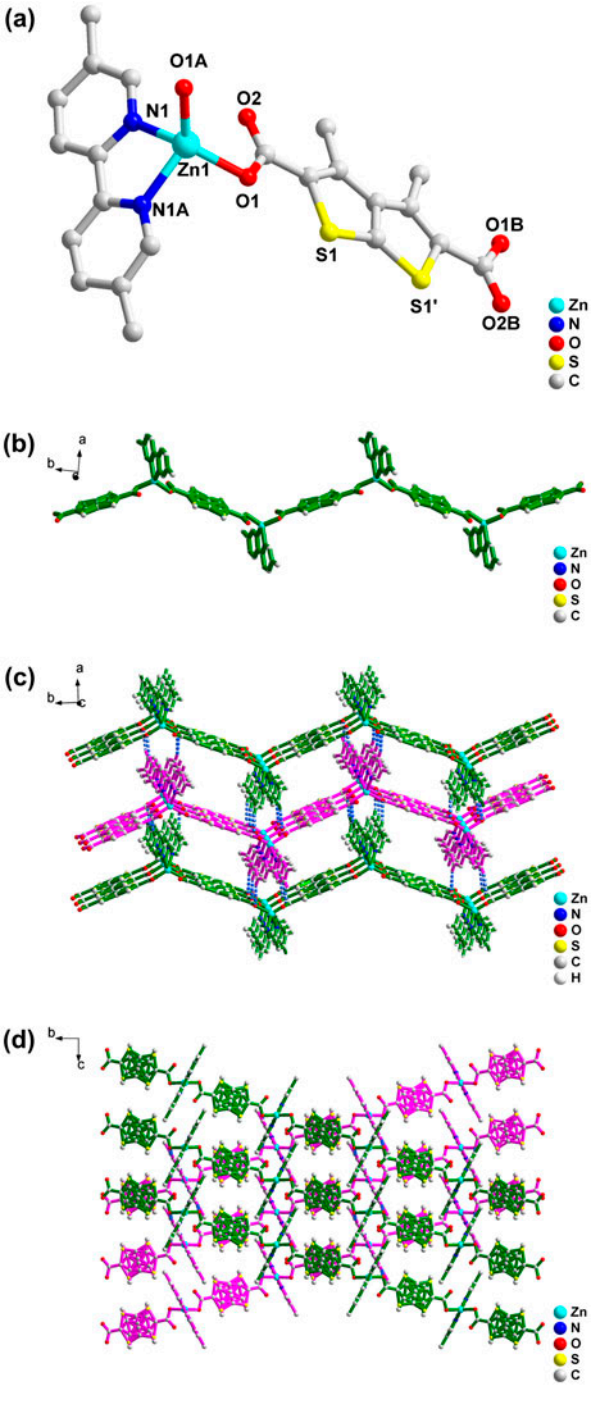

Figure 2. (a) Local coordination environment of **2**. All hydrogens are omitted for clarity. Symmetry codes for the generated atoms: A: $x, -y+1/2, -z+3/2$; B: $-x+2, -y, -z+1$. (b) View of the zigzag chain structure of **2** along the *b*-axis. (c) and (d) View of the 3-D supramolecular structure of **2** along the *c*- and *a*-axes, respectively, showing the special stacking mode of the chains.

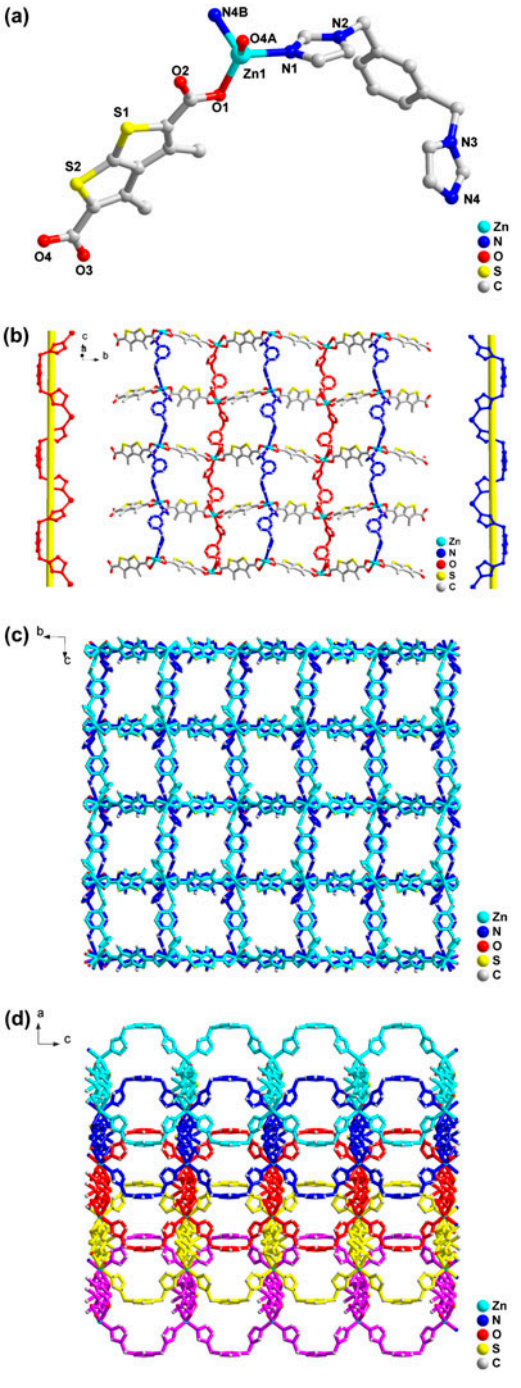

Figure 3. (a) Local coordination environment of **3**. All hydrogens are omitted for clarity. Symmetry codes for the generated atoms: A: $-x+1/2$, $y-1/2$, z; B: x, $-y+1/2$, $z+1/2$. (b) View of the 2-D conjugated layer of **3** showing the connectivity of the Zn-bimb chains. (c) and (d) View of the 3-D supramolecular structure along the *a*-axis and *b*-axis, respectively.

4.3. *Description of {[Zn(DMTDC)(1,3-bimb)]·2DMF·H_2O}$_n$ (3)*

Compound **3** crystallizes in the space group *Pbca* with orthorhombic crystal system and features a 2-D highly conjugated layer structure. The asymmetric unit contains one Zn(II), one $DMTDC^{2-}$, one 1,3-bimb, one H_2O, and two lattice DMF molecules. As described in figure 3(a), Zn(II) also adopts four-coordinate tetrahedral geometry with two carboxylate oxygens (O1 and O4A) from two different $DMTDC^{2-}$ ligands and two nitrogens (N1 and N4B) of two 1,3-bimb ligands. The Zn–O and Zn–N bond lengths lie in the normal range of 1.987(3)–2.034(4) Å. 1,3-bimb ligands in *GC* conformation connect adjacent Zn(II) centers to form infinite 1-D helical chains along the *c*-axis, which are further linked by (κ^0-κ^1)-(κ^0-κ^1)-μ_2 $DMTDC^{2-}$ anion ligands to generate a corrugated helical monolayer along the *bc* plane [figure 3(b)]. Within the layer, adjacent Zn-bimb–Zn-bimb helices exhibit opposite helicity and both right and left helices extend the 2_1-helical axis with a pitch of 23.32(1) Å. As a result, the whole crystal is mesomeric and does not exhibit chirality. The dihedral angle between the two imidazole rings is 67.9°. Topologically, the 2-D layer can be viewed as a (4,4) network with both $DMTDC^{2-}$ and 1,3-bimb ligands acting as bidentate linkers. The window size of the grid is 11.66(4) × 12.65(1) Å based on the Zn···Zn distances. Adjacent layers further interacted with each other through weak interactions between the aromatic rings along the *a*-axis [figure 3(c) and (d)]. 1-D channels are generated, which are filled with disordered DMF and H_2O molecules (figure S3). The potential solvent-accessible volume in the unit cell is 2859.0 Å^3, which accounts for 40.8% of the total cell volume as calculated by PLATON.

5. Properties

5.1. *PXRD diffractions and TGA*

PXRD diffractions of **1–3** are shown in figures S4–S6. All the peaks measured were similar to those in the simulated patterns, indicating the purity of all the compounds. TGA were performed on **1–3** to investigate the thermal stability of these polymers (figure S7). The TGA curve of **1** displays steady weight loss from 150 to 230 °C

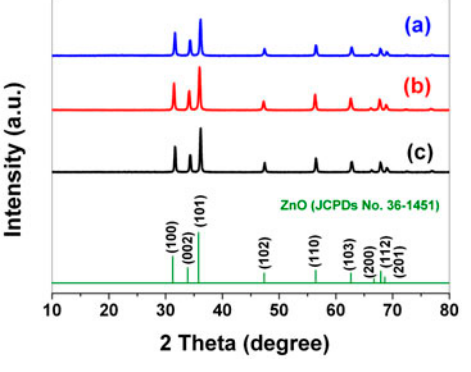

Figure 4. XRD patterns of the products by solid-state decomposition of (a) **1**, (b) **2**, and (c) **3**, respectively.

(found 3.6%), corresponding to the loss of coordinated H_2O (Calcd 3.4%). The decomposition of the whole structure corresponds to the rapid weight loss from 380 to 600 °C. For **2**, the loss of the lattice DMF and H_2O molecules (Calcd 10.7%) occurs at 130–200 °C (found 11.3%) and the rapid weight loss in the temperature range 300–350 °C indicates decomposition of the structure. The curve of **3** displays rapid weight loss from 150 to 270 °C from loss of lattice DMF and H_2O molecules (Calcd 22.7%, found 23.0%). No weight loss occurred until 600 °C, indicating the decomposition of the whole structure from then on. To identify the decomposition products of all compounds, TEM and XRD measurements were performed. As shown in

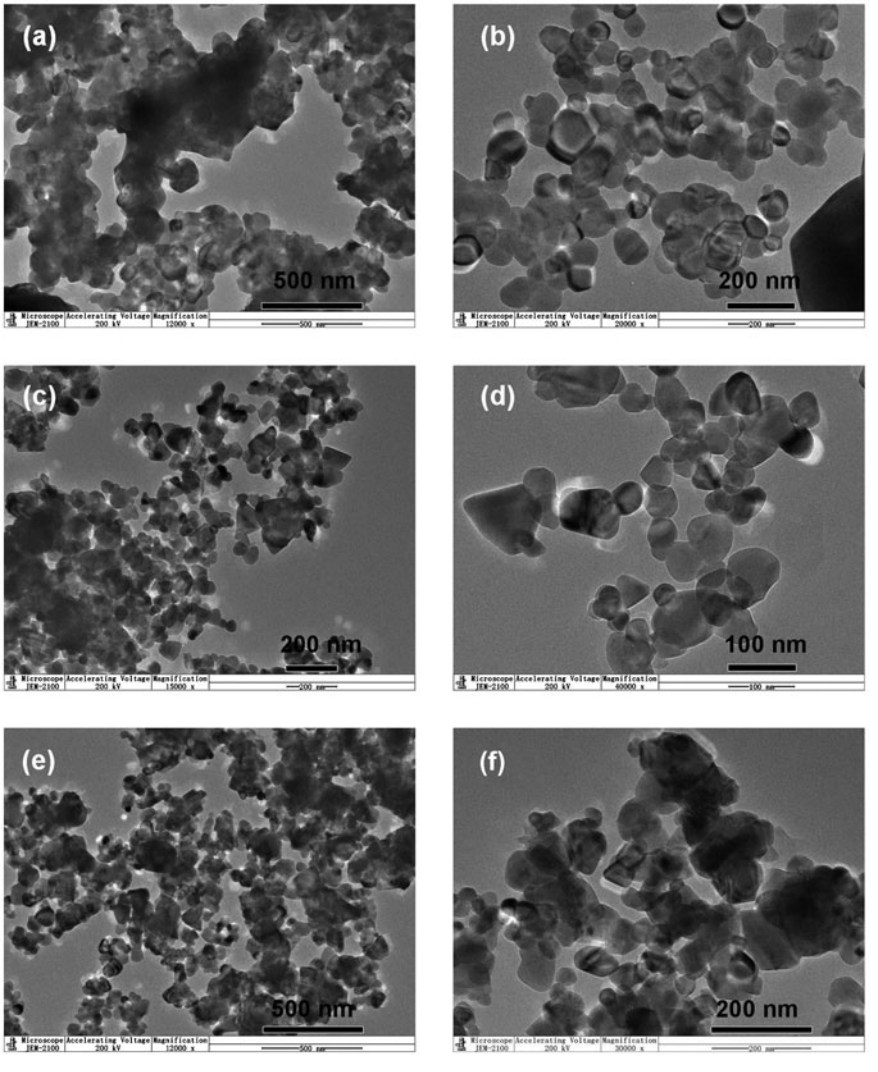

Figure 5. TEM images of the products by solid-state decomposition of **1** ((a) and (b)); **2** ((c) and (d)); and **3** ((e) and (f)).

figures 4 and 5, all the decomposition products display pure phase ZnO nanoparticles with diameter of 60–120 nm.

5.2. *Photoluminescent properties*

The photoluminescence spectra of the compounds and free ligands were measured in the solid state at room temperature (figures 6 and S8). H_2DMTDC and 1,3-bimb show almost no emission. 5,5′-dmbpy and 1,3-bimb show emission peaks at 577 nm (λ_{ex} = 340 nm) and 570 (λ_{ex} = 368 nm), respectively. These emissions may be ascribed to the intraligand $\pi \rightarrow \pi^*$ or $\pi^* \rightarrow n$ transitions [29, 30]. Compounds **1** and **3** display similar emission behaviors with respective maxima at 435 nm (λ_{ex} = 338 nm) and 467 nm (λ_{ex} = 367 nm), respectively. Zn(II) and Cd(II) ions are difficult to oxidize or to reduce. As a result, the emission bands should be ascribed to neither MLCT nor LMCT, but intraligand transitions [31–33]. Blue shift of the spectra may be attributed to ligation of the ligand to the metal center. The coordination enhances the "rigidity" of the ligand and thus reduces the loss of energy through a radiationless pathway [34, 35]. The difference of the peaks and intensity may result from different metal centers, ligands with different coordination and conformations. Additionally, weak interactions, especially $\pi \cdots \pi$ stacking interactions in the crystalline lattice, may affect the rigidity of the whole network and further the energy transfer involved in luminescence [36–39].

To examine the potential sensing of small solvent molecules, fluorescent properties of the ligand and compounds were investigated in different solvents. The suspensions were prepared by introducing 2 mg of finely ground sample of the ligand and **1–3** into 4 mL solvents, including methanol, ethanol, acetonitrile, dichloromethane, and tetrahydrofuran. Before measurements, the suspension was treated with ultrasonication for 30 min. As shown in figure 7, the luminescence intensities depend on different solvent molecules for different compounds. This may be attributed to interactions of the solvents with some sites of the compounds, which can influence the energy transfer process [36, 40–43].

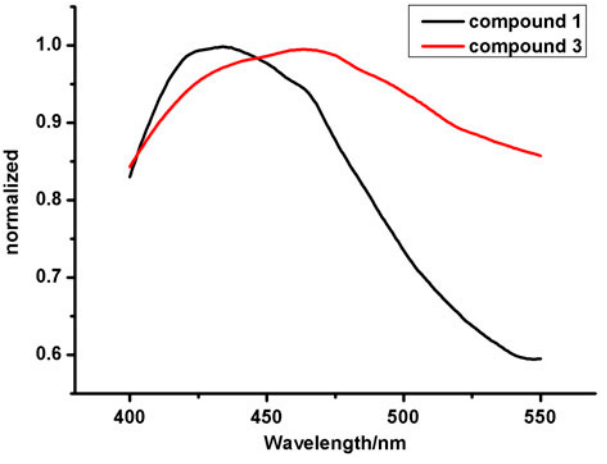

Figure 6. Solid-state photoluminescence properties of **1** and **3** at room temperature.

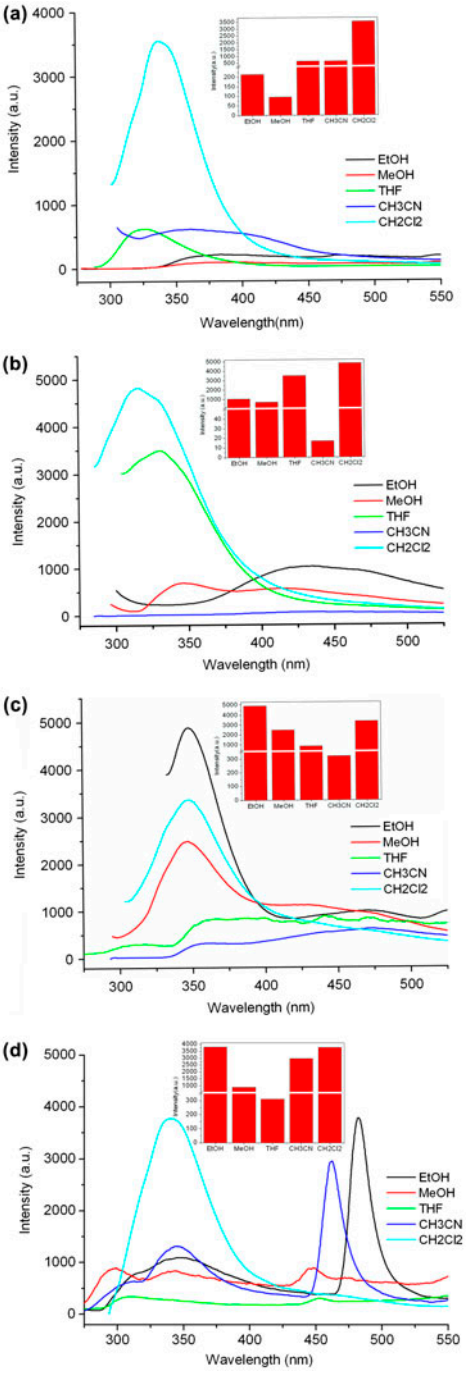

Figure 7. Emission spectra of (a) DMTDC (λ_{ex} = 286 nm) and compounds; (b) **1** (λ_{ex} = 283 nm); (c) **2** (λ_{ex} = 273 nm); and (d) **3** (λ_{ex} = 235 nm) in different solvents.

6. Conclusion

Three zinc coordination compounds were hydrothermally obtained from a bithiophene dicarboxylate. The N-donor co-ligands affect the resulting structures. The compounds and ligands exhibit photoluminescent properties at room temperature.

Supplementary material

X-ray crystallographic files in CIF format, additional tables and figures, XRD, TG, and photoluminescent spectra are available in supporting material section. The CCDC reference numbers 983015, 983016, and 983014 are for **1**–**3**, respectively. These data can be obtained free of charge from the Cambridge Crystallographic Data Center via www.ccdc.cam.ac.uk/data_request/cif.

Funding

We are thankful to the National Natural Science Foundation of China [grant number 20801025], [grant number 21101086], the Natural Science Foundation of Shandong Province [grant number ZR2012BQ023], and the University Scientific Research Development Plan of the Education Department of Shandong Province [grant numbet J14LC10].

References

[1] D. Zhao, D.J. Timmons, D. Yuan, H.-C. Zhou. *Acc. Chem. Res.*, **44**, 123 (2011).
[2] S. Chaemchuen, N.A. Kabir, K. Zhou, F. Verpoort. *Chem. Soc. Rev.*, **42**, 9304 (2013).
[3] M. Du, C.-P. Li, C.S. Liu, S.M. Fang. *Coord. Chem. Rev.*, **257**, 1282 (2013).
[4] H.-L. Jiang, T.A. Makal, H.-C. Zhou. *Coord. Chem. Rev.*, **257**, 2232 (2013).
[5] D.-S. Li, Y.-P. Wu, J. Zhao, J. Zhang, J.Y. Lu. *Coord. Chem. Rev.*, **261**, 1 (2014).
[6] J.-C. Jin, W.-Q. Tong, C.-G. Xie, W.-G. Chang, G.-N. Xu, J. Wu, L.-G. Li, Z.-Q. Yan, Y.-Y. Wang. *J. Coord. Chem.*, **66**, 3697 (2013).
[7] J.-J. Wang, Q.-L. Bao, J.-X. Chen. *J. Coord. Chem.*, **66**, 2578 (2013).
[8] P.-F. Yao, C.-J. Ye, F.-P. Huang, H.-D. Bian, Q. Yu, K. Hu. *J. Coord. Chem.*, **66**, 1591 (2013).
[9] N.L. Rosi, J. Kim, M. Eddaoudi, B. Chen, M. O'Keeffe, O.M. Yaghi. *J. Am. Chem. Soc.*, **127**, 1504 (2005).
[10] Z. Chen, B. Zhao, P. Cheng, X.-Q. Zhao, W. Shi, Y. Song. *Inorg. Chem.*, **48**, 3493 (2009).
[11] Y. Takashima, C. Bonneau, S. Furukawa, M. Kondo, R. Matsuda, S. Kitagawa. *Chem. Commun.*, **46**, 4142 (2010).
[12] I.A. Ibarra, S. Yang, X. Lin, A.J. Blake, P.J. Rizkallah, H. Nowell, D.R. Allan, N.R. Champness, P. Hubbersteya, M. Schröder. *Chem. Commun.*, **47**, 8304 (2011).
[13] R. Sibille, T. Mazet, E. Elkaïm, B. Malaman, M. François. *Inorg. Chem.*, **52**, 608 (2013).
[14] J.C. Rowsell, O.M. Yaghi. *J. Am. Chem. Soc.*, **128**, 1304 (2006).
[15] S. Bureekaew, H. Sato, R. Matsuda, Y. Kubota, R. Hirose, J. Kim, K. Kato, M. Takata, S. Kitagawa. *Angew. Chem. Int. Ed.*, **49**, 7660 (2010).
[16] J. Zhao, X.-L. Wang, X. Shi, Q.-H. Yang, C. Li. *Inorg. Chem.*, **50**, 3198 (2011).
[17] S. Wang, S. Xiong, L. Song, Z. Wang. *CrystEngComm.*, **11**, 896 (2009).
[18] S. Wang, S. Xiong, Z. Wang, J. Du. *Chem. Eur. J.*, **17**, 8630 (2011).
[19] G.-S. Yang, Z.-L. Lang, H.-Y. Zang, Y.-Q. Lan, W.-W. He, X.-L. Zhao, L.-K. Yan, X.-L. Wang, Z.-M. Su. *Chem. Commun.*, **49**, 1088 (2013).
[20] S.-N. Wang, H. Xing, Y.-Z. Li, J. Bai, M. Scheer, Y. Pan, X.-Z. You. *Chem. Commun.*, 2293, (2007).
[21] S.-N. Wang, R. Sun, X.S. Wang, Y.-Z. Li, Y. Pan, J. Bai, M. Scheer, X.-Z. You. *CrystEngComm.*, **9**, 1051 (2007).
[22] R. Sun, S. Wang, H. Xing, J. Bai, Y. Li, Y. Pan, X. You. *Inorg. Chem.*, **46**, 8451 (2007).
[23] S. Wang, R. Yun, Y. Peng, Q. Zhang, J. Lu, J. Dou, J. Bai, D. Li, D. Wang. *Cryst. Growth Des.*, **12**, 79 (2012).
[24] S.H. Mashraqui, H. Hariharasubrahmanian, S. Kumar. *Synthesis*, **12**, 2030 (1999).

[25] *SAINT (Version 6.02a)*, Bruker AXS Inc., Madison, Wisconsin, USA (2002).
[26] G.M. Sheldrick. *SADABS, Program for Brucker Area Detector Absorption Correction*, Göttingen University, Germany (1997).
[27] G.M. Sheldrick. *SHELXS-97, Program for Crystal Structure Solution*, Göttingen University, Germany (1997); G.M. Sheldrick. *SHELXL-97, Program for Crystal Structure Refinement*, Göttingen University, Germany (1997).
[28] A.L. Spek. *J. Appl. Crystallogr.*, **36**, 7 (2003).
[29] Y.-N. Zhang, P. Liu, Y.-Y. Wang, L.-Y. Wu, L.-Y. Pang, Q.-Z. Shi. *Cryst. Growth Des.*, **11**, 1531 (2011).
[30] X.-L. Li, G.-Z. Liu, L.-Y. Xin, L.-Y. Wang. *CrystEngComm.*, **14**, 1729 (2012).
[31] M.D. Allendorf, C.A. Bauer, R.K. Bhakta, R.J.T. Houk. *Chem. Soc. Rev.*, **38**, 1330 (2009).
[32] Z. Chang, A.-S. Zhang, T.-L. Hu, X.-H. Bu. *Cryst. Growth Des.*, **9**, 4840 (2009).
[33] L.-Y. Xin, G.-Z. Liu, X.-L. Li, L.-Y. Wang. *Cryst. Growth Des.*, **12**, 147 (2012).
[34] X.-L. Wang, C. Qin, E.-B. Wang, L. Xu, Z.-M. Su, C.-W. Hu. *Angew. Chem. Int. Ed.*, **43**, 5036 (2004).
[35] J. Zhang, Y.-R. Xie, Q. Ye, R.-G. Xiong, Z.-L. Xue, X.-Z. You. *Eur. J. Inorg. Chem.*, 2572 (2003).
[36] Y.-J. Cui, Y.-F. Yue, G.-D. Qian, B.-L. Chen. *Chem. Rev.*, **112**, 1126 (2012).
[37] Y.-J. Mu, G. Han, S.-Y. Ji, H.-W. Hou, Y.-T. Fan. *CrystEngComm.*, **13**, 5943 (2011).
[38] X.-X. Zhou, H.-C. Fang, Y.-Y. Ge, Z.-Y. Zhou, Z.-G. Gu, X. Gong, G. Zhao, Q.-G. Zhan, R.-H. Zeng, Y.-P. Cai. *Cryst. Growth Des.*, **10**, 4014 (2010).
[39] S. Wang, H. Xing, Y. Li, J. Bai, Y. Pan, M. Scheer, X. You. *Eur. J. Inorg. Chem.*, 3041 (2006).
[40] S. Pramanik, C. Zheng, X. Zhang, T.J. Emge, J. Li. *J. Am. Chem. Soc.*, **133**, 4153 (2011).
[41] H. Wang, W.-T. Wang, Z.M. Sun. *Chem. -Asian J.*, **8**, 982 (2013).
[42] Y. Yang, P. Du, Y.-Y. Liu, J.-F. Ma. *Cryst. Growth Des.*, **13**, 4781 (2013).
[43] F.Y. Yi, W. Yang, Z.-M. Sun. *J. Mater. Chem.*, **22**, 23201 (2012).